

ORIGINAL ARTICLE

Physiology and genetic traits of reverse osmosis membrane biofilms: a case study with *Pseudomonas aeruginosa*

Moshe Herzberg¹ and Menachem Elimelech²¹Department of Desalination and Water Treatment, Zuckerman Institute for Water Research, Ben Gurion University, Sede-Boqer, Israel and ²Environmental Engineering Program, Department of Chemical Engineering, Yale University, New Haven, CT, USA

Biofilm formation of *Pseudomonas aeruginosa* on the surface of a reverse osmosis (RO) membrane was studied using a synthetic wastewater medium to simulate conditions relevant to reclamation of secondary wastewater effluent. *P. aeruginosa* biofilm physiology and spatial activity were analyzed following growth on the membrane using a short-life green fluorescent protein derivative expressed in a growth-dependent manner. As a consequence of the limiting carbon source prevailing in the suspended culture of the RO unit, a higher distribution of active cells was observed in the biofilm close to the membrane surface, likely due to the higher nutrient levels induced by concentration polarization effects. The faster growth of the RO-sessile cells compared to the planktonic cells in the RO unit was reflected by the transcriptome of the two cultures analyzed with DNA microarrays. In contrast to the findings recently reported in gene expression studies of *P. aeruginosa* biofilms, in the RO system, genes related to stress, adaptation, chemotaxis and resistance to antibacterial agents were induced in the planktonic cells. In agreement with the findings of previous *P. aeruginosa* biofilm studies, motility- and attachment-related genes were repressed in the RO *P. aeruginosa* biofilm. Supported by the microarray data, an increase in both motility and chemotaxis phenotypes was observed in the suspended cells. The increase in nutrient concentration in close proximity to the membrane is suggested to enhance biofouling by chemotaxis response of the suspended cells and their swimming toward the membrane surface.

The ISME Journal (2008) 2, 180–194; doi:10.1038/ismej.2007.108; published online 29 November 2007

Subject Category: microbial engineering

Keywords: biofouling; reverse osmosis; biofilms; *Pseudomonas aeruginosa*

Introduction

Attachment of bacteria and biofilm formation on membrane surfaces are major impediments to the efficient operation of reverse osmosis (RO) membrane systems commonly used in reclamation of wastewater and desalination of sea water. Once bacteria deposit onto the membrane, even a slight amount of nutrients is sufficient to allow the cells to multiply and produce extracellular polymeric substances (EPSs) (Ridgway and Flemming, 1996). Bacterial biofilms are well-organized structured communities (Costerton *et al.*, 1995), and once a biofilm is present on an RO membrane surface, membrane performance deteriorates. Biofilm growth

on RO membranes results in permeate water flux decline and, in most cases, a decrease in salt rejection (Ridgway and Flemming, 1996).

Recently, we have shown that the biofouling layer on RO membranes has a dual mechanism for deteriorating membrane performance (Herzberg and Elimelech, 2007). The bacterial cells in the biofouling layer act as a particulate fouling layer, hindering back-diffusion of salts from the membrane surface, thus elevating the osmotic pressure near the membrane surface. On the other hand, the EPS component of the biofouling layer seems to mainly increase the biofilm hydraulic resistance to permeate flow. The increase in both the transmembrane osmotic pressure and the hydraulic resistance of the biofilm act together to decrease permeate water flux.

It is now well accepted that biofilm formation by *Pseudomonas aeruginosa* is a developmental process that involves four main stages: bacterial deposition and irreversible adhesion, formation of microcolonies, maturation and dispersion of the cells back to their planktonic stage (O'Toole *et al.*,

Correspondence: M Herzberg, Department of Desalination and Water Treatment, Zuckerman Institute for Water Research, Ben Gurion University, Sede-Boqer Campus, 84990, Israel.

E-mail: herzberg@bgu.ac.il

Received 7 August 2007; accepted 26 October 2007; published online 29 November 2007

2000; Sauer *et al.*, 2002, 2004). Recent studies show that biofilm formation is a highly regulated process with different genes being expressed at different stages (Southey-Pillig *et al.*, 2005; Waite *et al.*, 2006).

Irreversible adhesion (attachment) of the bacterial cells to the surface is mediated by biological, physical and chemical factors (Donlan, 2002). These include substratum properties (such as roughness and hydrophobicity), a 'conditioning film' of macromolecules on the surface, system hydrodynamics, medium characteristics (such as ionic strength, pH and the presence of multivalent cations) and cell surface properties (such as hydrophobicity, expression of flagella and pili, lipopolysaccharides and EPS).

The next biofilm formation stage takes place by auto-aggregation of the attached cells and formation of microcolonies (Ramsey and Whiteley, 2004). In *P. aeruginosa* for example, this process is mediated by surface translocation through twitching motility, attributed to type IV pili (O'Toole *et al.*, 2000). Proliferation of *Escherichia coli* on the surface and formation of microcolonies are ascribed to type I pili and to the self-recognizing surface adhesin, the autotransporter protein Antigen 43 (Danese *et al.*, 2000; Schembri *et al.*, 2001).

Following attachment, EPS synthesis is increased, creating a three-dimensional structure within the biofilm community (Branda *et al.*, 2005). The main polysaccharides in *E. coli* biofilms include colanic acid and β -1,6-*N*-acetyl-D-glucosamine (Wang *et al.*, 2004). For *P. aeruginosa* biofilms, the main polysaccharides are alginate and other glucose- and mannose-rich polysaccharide components (Friedman and Kolter, 2004; Jackson *et al.*, 2004). This maturation stage has been shown to be accompanied by the development of antibiotic resistance by the biofilm cells (Drenkard, 2003).

The last stage in biofilm formation is cell detachment. Cell detachment is an active form of dispersion of cells from the biofilm matrix (Romeo, 2006), as opposed to physical shearing of cell aggregates often described as sloughing events (Donlan, 2002). During this step of the biofilm formation cycle, subpopulations of detached mature biofilm cells reinitiate biofilm formation on new sites. While the mechanisms of cell dispersion are not fully understood, cell dispersion has been linked to changes in nutrient levels (Sauer *et al.*, 2004) and to quorum sensing (Liu *et al.*, 2007).

Quorum sensing has been linked to biofilm formation for almost a decade, when the first signal shown to affect biofilm was *N*-(3-oxododecanoyl)-L-homoserine lactone in *P. aeruginosa* biofilms (Davies *et al.*, 1998). Since then, quorum sensing has been linked to biofilm formation at all stages—attachment, auto-aggregation, maturation and dispersal (Hammer and Bassler, 2003; Parsek and Greenberg, 2005). However, the effects of disrupting quorum-sensing signals on biofilm formation and maintenance are strain and media dependent (Kirisits and Parsek, 2007), and in many cases, offer

no conclusive information that can be used to control biofilms in engineered systems.

Once bacteria attach to a surface, they undergo changes in gene expression, which influence cell physiology and phenotypes. *P. aeruginosa* was shown to induce *algC*, a gene involved in alginate biosynthesis, as the cells attach to the surface (Davies *et al.*, 1993). In *P. aeruginosa*, pili- and flagella-related genes that are involved in attachment to the surface (O'Toole and Kolter, 1998) are repressed in the maturation stage (Whiteley *et al.*, 2001). Also, in *P. putida*, flagella-related genes were repressed 6 h after cell attachment (Sauer and Camper, 2001). Flagella were also shown to be important at the dispersion stage of *P. aeruginosa* biofilms (Sauer *et al.*, 2002). Recently, temporal changes in protein expression were observed in a *P. aeruginosa* biofilm during its maturation and dispersion stages (Southey-Pillig *et al.*, 2005). During the maturation stages, proteins involved in virulence, adaptation, antibiotic resistance, nitrification and quorum sensing were induced in the biofilm. It was also shown that quorum-related multi-drug efflux pumps were induced during biofilm formation (Southey-Pillig *et al.*, 2005). These efflux pumps were postulated to play a role in antibiotic resistance mechanisms. Since bacteria in the biofilm matrix are likely to face nutrient limitation and various stress conditions, the stationary-phase sigma factor, RpoS, is likely to be expressed to a higher degree than the associated suspended cells, as shown previously by Waite *et al.* (2006) and Xu *et al.* (2001).

Understanding the main genetic traits in RO biofilms may help to develop strategies for controlling biofilms in RO systems. In general, the lower susceptibility of biofilm cells to antimicrobial agents is mainly attributed to the lower growth rate of biofilm cells and to related changes in cell physiology (Stewart, 2002; Shah *et al.*, 2006). It is of utmost importance to analyze how the growth rate of sessile cells on RO membranes is affected by different environmental conditions, in comparison to the planktonic cells in the system. Under conditions in which there are limited dissolved substrates for growth, the elevated concentration polarization of salts and nutrients on RO membranes may enhance cell growth rate, and may affect the susceptibility of the attached cells to antibacterial agents.

Membrane biofilm physiology can be discerned either by analyzing metabolic state and activity through measuring the amount of adenosine 5'-triphosphate (ATP) or by analyzing electron-transport activity through staining with the redox-sensitive dye, 5-cyano-2,3-ditolyl tetrazolium chloride (Ridgway and Flemming, 1996). 5-Cyano-2,3-ditolyl tetrazolium chloride has also been used to measure the effect of biocides on biofilms formed on simulated membrane surfaces (Ridgway and Flemming, 1996). In contrast to the extensive studies in the past four decades on the physiology of bacterial

biofilms on solid surfaces, studies on membrane biofilm physiology are scarce. In biofilm research, major advances in molecular science, such as proteomics, genomics, and gene and protein expression, are already being used extensively. However, the above methodologies have not yet been applied to membrane biofilms, especially in RO.

The overall objective of this study was to characterize biofilm physiology on RO membranes. We accomplished this by (i) studying the dynamics of biofilm formation on RO membranes, (ii) relating the growth-limiting nutrients in the media to the spatial activity of the biofilm and (iii) analyzing the main genetic traits of a model bacterium, *P. aeruginosa* PAO1, in the biofouling layer and the suspended culture in the RO unit. Well-controlled, short-term biofouling experiments with *P. aeruginosa* PAO1 were conducted using a laboratory-scale RO test unit and an enriched synthetic wastewater medium to simulate conditions relevant to reclamation of secondary effluent. Using a laser scanning confocal microscope (LSCM) and a short-life green fluorescent protein (GFP)-tagged *P. aeruginosa* PAO1 controlled by a growth-dependent promoter, we observed biofilm spatial growth on the RO membrane surface. In addition, differential gene expression of the RO *P. aeruginosa* biofilm analyzed by Affymetrix DNA microarray technology further confirmed differences in growth patterns between the suspended and the RO membrane-sessile cells.

Materials and methods

Bacterial strains and growth media

A derivative of *P. aeruginosa* PAO1 chromosomally encoding short-life GFP, PAO1 AH298, was kindly received from S Molin (Werner *et al.*, 2004), at the Technical University of Denmark. This strain is tellurite resistant ($150 \mu\text{g ml}^{-1}$) and its GFP expression is growth dependent due to the *rrnBp₁* promoter located upstream of the *gfp* gene. A fresh single colony of PAO1 AH298 (pre-grown on Luria-Bertani (LB) agar supplemented with tellurite) was used as inoculum for an overnight culture grown in LB broth. This overnight culture was re-diluted in LB broth and allowed to grow to late exponential phase with a final optical density (600 nm) of 1 for use as inoculum for the biofouling experiments. For total RNA isolation, to be used in the microarray analysis, the wild-type strain, *P. aeruginosa* PAO1, was grown to a final optical density (600 nm) of 1 and inoculated in the RO unit for growth of biofilm and suspended cells as described later in this section.

An enriched synthetic wastewater medium was used for bacterial growth in the RO crossflow test unit. The chemical composition chosen for the synthetic wastewater was based on secondary effluent quality from selected treatment plants in California with high-rate biological processes

(Pettygrove and Asano, 1984). To achieve an enhanced biofouling behavior, a relatively high-concentration of carbon and energy source, together with a 1:1000 dilution of LB broth, was supplemented to the wastewater media. Specifically, to prepare the synthetic wastewater, deionized water (DI) (Nano Pure II; Barnstead, Dubuque, IA, USA) was supplemented as follows: 1.16 mM sodium citrate, 0.94 mM NH_4Cl , 0.45 mM KH_2PO_4 , 0.5 mM $\text{CaCl}_2 \cdot 2\text{H}_2\text{O}$, 0.5 mM NaHCO_3 , 2.0 mM NaCl and 0.6 mM $\text{MgSO}_4 \cdot 7\text{H}_2\text{O}$. In addition, 1 ml of LB broth was added per 1 l of solution. The final pH was 7.4 and the calculated total ionic strength was 14.6 mM. All chemicals were American Chemical Society (ACS) grade (Fisher Scientific, Pittsburgh, PA, USA).

RO membrane, crossflow test unit and biofouling protocol

A commercial thin film composite RO membrane, LFC-1 (Hydranautics, Oceanside, CA, USA), was used as a model membrane for the biofouling experiments. The hydraulic resistance of the membrane was determined to be $1.06 (\pm 0.018) \times 10^{14} \text{ m}^{-1}$ at 25 °C. The observed salt passage was $2.11 \pm 0.44\%$ (or 97.89% salt rejection), as determined by electric conductivity using the synthetic wastewater described above at an applied pressure of 180 p.s.i. (1241 kPa) and a crossflow velocity of 8.5 cm s^{-1} . The membrane was received as a flat sheet and stored in DI water at 4 °C. Physical and chemical properties of the LFC-1 membrane can be found in our previous publication (Vrijenhoek *et al.*, 2001).

A laboratory-scale test unit, similar to that described in our previous publication (Ang *et al.*, 2006) was used for the biofouling experiments. The unit was comprised of a membrane crossflow cell, high-pressure pump (Hydra-Cell; Wanner Engineering Inc., Minneapolis, MN, USA), feed water reservoir, chiller equipped with a temperature control system (Neslab RTE-7, Thermo Electron) and a data acquisition system (PC interfaced) used to acquire the permeate flow rate (Optiflow 1000 flowmeter; Humonics, Folsom, CA, USA), conductivity (Accumet AR60; Fisher Scientific) and dissolved oxygen concentration (Accumet AR60; Fisher Scientific). The retentate flow rate was monitored with a floating disk rotameter (King Instrument, Fresno, CA, USA). The dimensions of the rectangular, crossflow membrane channel were $7.7 \text{ cm} \times 2.6 \text{ cm}$, with a channel height of 0.3 cm. Both permeate and retentate were recirculated back to the feed reservoir, limiting the well-controlled biofouling experiments to short time periods of batch growth conditions.

A biofouling protocol, described in our recent publication (Herzberg and Elimelech, 2007), allowed bacterial deposition and growth on the membrane surface. Briefly, before every experiment and prior to inserting the RO membrane coupon, the RO unit was disinfected and thoroughly cleaned to

remove microorganisms and trace organic impurities by applying the following steps: (1) recirculation of 0.5% sodium hypochlorite for 2 h, (2) rinsing the unit twice by recirculating tap water for 10 min, (3) recirculation of 5 mM EDTA at pH 11 for 30 min, (4) repeating step 2, (5) additional cleaning of trace organic matter by recirculation of 2 mM sodium dodecyl sulfate (SDS) at pH 11 for 30 min, (6) repeating step 2, (7) sterilizing the unit by recirculation of 95% ethanol for 1 h, (8) rinsing the unit three times with DI water (heterotrophic count of the DI water was less than 10 bacterial cells per ml) to eliminate ethanol residues and (9) inserting the LFC-1 membrane coupon.

Following the sterilization/cleaning protocol, the membrane was compacted with DI water at a pressure of 300 p.s.i. (2068 kPa) until the permeate flux attained a constant value (usually after 12–18 h). Following compaction of the membrane, a 1 h baseline performance with DI water at 180 p.s.i. (1241 kPa) at 25 °C (corresponding to initial permeate flux of $1.18 \times 10^{-5} \text{ m s}^{-1}$ or $42.5 \text{ l m}^{-2} \text{ h}^{-1}$) was conducted, with this pressure and temperature being maintained during all the experiments. After attaining a stable flux with DI water, the previously described synthetic wastewater was added to the feed reservoir, excluding the 1 ml LB broth per liter of media and the 0.94 mM NH_4Cl . The system was equilibrated for 5 h with this electrolyte solution. After this stage, a culture of *P. aeruginosa* PAO1 (either the wild type or its *gfp* derivative, PAO1 AH298) was washed three times with an electrolyte solution identical to the one used in the fouling experiments. Suspended cells (10 ml) (late exponential growth phase), with a final optical density (600 nm) of 1, were centrifuged for 10 min at 8000 r.p.m. and 4 °C, and re-suspended by vortexing. The washed exponential phase culture was inoculated into the feed reservoir to achieve an initial cell concentration of 10^7 cells per ml. The bacteria were recirculated within the unit, allowing cell deposition to occur on the RO membrane for 30 min, followed by the addition of LB and ammonium chloride. Samples from the permeate and the feed reservoir were collected at all stages for determination of total organic carbon (TOC) and conductivity. Oxygen concentrations in the feed reservoir during the experiments varied between 3.2 and 3.5 mg l^{-1} .

Laser scanning confocal microscopy and image analysis

At the end of each biofouling experiment with *P. aeruginosa* PAO1 AH298, the membrane coupon was carefully removed and cut into pieces of 5 mm × 5 mm for staining with either concanavalin A (ConA) conjugated to tetramethylrhodamine isothiocyanate (TRITC) or with propidium iodide (PI), for probing EPS or dead cells, respectively. Microscopic observation and image acquisition were performed using an LSCM (Zeiss—Axiovert 10),

equipped with Zeiss dry objective Plan-NeoFluar ($\times 10$ magnification and a numerical aperture of 0.3). The LSCM was equipped with detectors and filter sets for monitoring PI/TRITC-stained cells and GFP (excitation wavelengths of 568 and 488 nm, respectively). LSCM images were generated using the Bio-Rad confocal assistant software (version 4.02). Gray scale images were analyzed, and both specific biovolume ($\mu\text{m}^3/\mu\text{m}^2$) and viable/dead cell distribution in the biofouling layer were determined by COMSTAT, an image-processing software (Heydorn *et al.*, 2000), written as a script in Matlab 5.1 (The MathWorks, Natick, MA, USA) and equipped with an image-processing toolbox. Thresholding was fixed for all image stacks. For each time point, between six and nine positions on the membrane were chosen and microscopically observed and analyzed.

The ConA, conjugated to TRITC (Invitrogen Co., Carlsbad, CA, USA), was used as a probe to determine the presence of PAO1 EPS (Strathmann *et al.*, 2002). Briefly, frozen (−20 °C) 100 μl aliquots of 1 mg ml^{-1} labeled ConA stock solution were prepared in 10 mM phosphate buffer (pH 7.5) and diluted to 100 $\mu\text{g ml}^{-1}$ prior to use in 10 mM phosphate buffer (pH 7.5). Excess electrolyte solution was carefully drawn off from two pieces of a biofilm-covered membrane by gently touching the edge of the specimens with a tissue paper (Kim-wipes). Then, 100 μl of ConA staining solution was added to cover the biofilm samples, which were then incubated in the dark, at room temperature for 20 min. Unbound ConA was drawn off from the specimens using a three-step wash of 10 mM phosphate buffer. The unbound ConA solution and the washing solution were carefully removed by gently touching the edge of the specimen with a tissue paper.

PI was used for probing dead cells in the biofouling layer. Excess electrolyte solution was carefully drawn off from a piece of a biofilm-covered membrane in the same manner used for ConA staining. Then, 100 μl of 3 μM PI solution (prepared in 10 mM phosphate buffer, pH 7.5) was added to cover the biofilm samples, which were then incubated in the dark at room temperature for 20 min. Excess PI solution was carefully drawn off with tissue paper. The excess PI nucleic acid stain that did not bind to the biofilm samples was then removed by rinsing three times with a 10 mM phosphate buffer at pH 7.5.

Dissolved organic carbon, oxygen concentration and conductivity measurements

Dissolved organic carbon analysis was conducted with a TOC analyzer (Shimadzu TOC-V CSH). Prior to analysis, 20 ml feed and permeate samples were filtered through a 0.22 μm syringe-sterilized polyvinylidene fluoride (PVDF) filter (Durapore). Dissolved oxygen concentrations were measured

continuously in a custom-made glass flow cell (50 ml) designed for a dissolved oxygen electrode (Fisher Scientific). The oxygen uptake rate (OUR) of the biofilm layer was calculated as the product of the permeate flow rate and the difference between oxygen concentration in the feed and the permeate solutions. To determine salt rejection, electrical conductivities of both the feed and permeate were measured with an Accumet conductivity electrode (four-cell type with a cell constant of 1.0 cm^{-1}).

Total RNA extraction from suspended and biofilm cells

Both suspended and biofilm cells were collected at the end of the biofouling experiment (after 20 h). Suspended cells (500 ml) were centrifuged in two cold (0°C) centrifuge tubes for 2 min at 4°C and 10 000 r.p.m., re-suspended into 4 ml of cold (0°C) NaCl solution (0.85%), and centrifuged for 15 s at 13 500 r.p.m. Biofilm cells were extracted from the membrane coupon by 2 min of sonication in a cold (0°C) 200 ml NaCl solution (0.85%), followed by 2 min of centrifugation at 4°C and 10 000 r.p.m. Then, the biofilm cells were re-suspended with 4 ml of cold (0°C) NaCl solution (0.85%) and centrifuged for 15 s at 13 500 r.p.m. in a chilled 2 ml-bead-beater centrifuge tube. Both suspended and biofilm pellets were immediately fast-frozen into liquid nitrogen and kept at -70°C until total RNA extraction was carried out.

For RNA extraction, cell pellets were supplemented with 1% solution of β -mercaptoethanol in a RLT buffer (Qiagen, Valencia, CA, USA) and with 150 μl of 0.1 mm zirconia/silica beads (Biospec Products, Bartlesville, OK, USA). Then, cells were lysed in a bead-beater (Biospec Products) for 30 s at maximum speed. After cell lysis in the bead-beater and centrifugation of the cell debris and the lysate (15 s at 13 500 r.p.m.), 800 μl of the supernatant was taken out and added to 445 μl ethanol (100%). An RNeasy mini kit (Qiagen) was used for the final steps of RNA extraction. An on-column DNA digestion was performed with DNase I, according to the manufacturer's instructions. The 260 nm optical density of an RNA diluted sample (1:25) was used to measure RNA quantity, and a ratio of A_{260}/A_{280} between 1.8 and 2.1 was used to define RNA purity. RNA integrity was visualized in a 1.4% agarose gel.

Microarray analysis

A whole genome chip of *Pseudomonas aeruginosa* PAO1 (Affymetrix, Santa Clara, CA, USA) was used to detect and compare the transcriptomes of the suspended and biofilm cells in the RO unit. Total RNA (10 μg) was used for synthesis of labeled cDNA fragments according to Affymetrix protocol. Briefly, random primers composed mainly from hexamers (Invitrogen) were used for a reverse transcription reaction to synthesize cDNA. The reaction mix was spiked with poly-adenylated transcripts of *Bacillus*

subtilis genes (*lys*, *phe*, *thr*, *dap*) (Poly-A controls) at different concentrations (Affymetrix). Spiking the reaction mix with Poly-A controls was used to monitor the performance and sensitivity of the arrays. The cDNA was fragmented with DNase I (Amersham Biosciences, Pittsburgh, PA, USA) in which cDNA fragments were identified in a 2% agarose gel, as a smear between 50 and 200 bp. Then, the 3' ends of the cDNA fragments were labeled with biotin bound-uracil using a terminal labeling kit (Enzo Life Sciences, Farmingdale, NY, USA). The biotin-labeled targets were hybridized to the *P. aeruginosa* PAO1 genome array (Affymetrix) for 16 h at 60 r.p.m. and 50°C using the hybridization oven model 640 (Affymetrix). A fluidics system model 450 (Affymetrix) was used for a three-step staining protocol. Streptavidin (Pierce Chemical, Rockford, IL, USA) was bound to the biotin residues on the hybridized fragments in the first staining step of the array. In the second staining step, a biotin-bound streptavidin antibody (Vector Laboratories) was added for signal enhancement. Finally, in the third step, a streptavidin fluorescently labeled with phycoerythrin (Molecular Probes, Carlsbad, CA, USA) was added for obtaining red fluorescent signals (emission at 570 nm) from the hybridized target.

A GeneChip scanner model 3000 (Affymetrix) was used for scanning the arrays. GeneChip operating software was used to generate a report indicating the signal intensities from each of the arrays, which were processed from either the suspended or the biofilm cells. In addition, a comparison file between the arrays was generated. The data were inspected for quality and analyzed according to the procedures described in Data Analysis Fundamentals (Affymetrix). To ensure the reliability of the induced/repressed gene list, genes were identified as differentially expressed if the *P*-value was less than 0.005 and the expression ratio was greater than 2 (GEO accession number GSE7266). The gene functions and annotations of *P. aeruginosa* PAO1 were obtained from the Pseudomonas Genome Database V2 (<http://www.pseudomonas.com/>) and from Windsor *et al.* (2005).

Motility assay

The motility assay was adapted from Sperandio *et al.* (2002). Biofilm culture (1 ml) was washed three times (8000 r.p.m., 2 min) in a chilled synthetic wastewater medium (0°C) as indicated in the previous section. Suspended culture (20 ml) was centrifuged for 2 min at 8000 r.p.m. and re-suspended in 1 ml of chilled synthetic wastewater medium (0°C), followed by two additional washing steps with a synthetic wastewater medium. Both optical densities (at 600 nm) of the suspended and the biofilm cells were adjusted to 1.0, after which a sterile toothpick was touched to the washed cultures (biofilm or suspended) and immediately pinched

between the motility plates. Fresh motility plates were prepared less than 6 h before the experiment. The plates contained 1% (w/v) tryptone, 0.25% (w/v) NaCl and 0.3% (w/v) agar. Motility halos were measured at 6 and 12 h. Between 8 and 10 plates were used to compare the motility between the biofilm and suspended cultures.

Chemotaxis assay

Chemotaxis assay was based on Adler's method (Adler, 1973). Biofilm and suspended cells were treated the same as before the motility assay. After washing the cells, 200 μ L of each of the cultures was added to a sterilized beaker with 20 ml of a synthetic wastewater medium without any carbon source. Four capillaries (Drummond Scientific Co., Broomall, PA, USA) were closed at one end and filled with 2 μ L of wastewater medium, which was supplemented with a chemo-attractant. The four capillaries were then submerged in the beaker with the wastewater medium. This procedure was repeated for each of the chemo-attractants and again for an additional four capillaries used for a control experiment, which was performed without chemo-attractant. After 1 h at room temperature, the capillaries were taken out, aseptically broken and diluted in 200 μ L of LB broth. Then, series of dilutions were prepared and spread on LB plates for enumerating the colonies the next day. The chemo-attractants used were L-serine at a concentration of 1 mM and citrate at a concentration of 10 mM. Chemotaxis response of the cells was defined as the ratio between cell concentration in the capillaries with chemo-attractant and cell concentration in the capillaries without chemo-attractant.

Results and discussion

Dynamics of biofilm growth and effect on membrane performance

Biofilm growth was monitored with LSCM for four experiments, which were terminated at different times—4, 10, 19 and 24 h—after inoculation of the bacteria. At the end of each of the biofouling experiments, the RO membrane coupon was carefully removed, and viable cells, dead cells and EPS were visualized by LSCM. Figure 1 presents representative LSCM image stacks after three-dimensional reconstruction with Imaris software (Bitplane, Zurich, Switzerland). A superposition of viable bacteria (expressing GFP) and EPS, probed with ConA conjugated to TRITC, is presented in Figure 1a. A superposition of viable bacteria and dead cells, probed with PI, is presented in Figure 1b. The specific biovolumes of the viable cells, dead cells, and EPS, calculated with COMSTAT software, are presented in Table 1. Initially, microcolonies of PAO1 were observed (4 h after PAO1 inoculation). Then, the biofouling layer grew to a thickness of approximately 20–30 μ m, where EPS was also

detected (10 and 19 h after PAO1 inoculation). After 19 and 24 h, more dead cells were observed. Crevices and holes in the biofouling layer were detected after 24 h, probably due to detachment of cells and small aggregates from the biofilm.

Biofilm formation is considered to be a developmental process, which begins with bacterial attachment to the surface, followed by auto-aggregation, microcolony formation, maturation and cell detachment. The rapid changes in biofilm structure observed here (Figure 1 and Table 1) do not follow the previously reported biofilm formation stages, which were observed over a much longer period of 4–6 days (Ramsey and Whiteley, 2004). Possible reasons for these rapid biofilm dynamics include a rapid initial cell deposition due to convective permeate flow through the membrane and the depletion of nutrients after 20–24 h in the RO unit. Furthermore, in previous reports (Ramsey and Whiteley, 2004; Boles *et al.*, 2005), rich growth media were used, while minimal media were applied in this study.

Permeate flux and salt rejection during the RO membrane biofouling started to decrease after 3–4 h of a lag phase (when permeate flux was still relatively constant), following the inoculation of bacteria in the RO unit (that is 9–10 h of the biofouling run). A drastic permeate flux decline and a concomitant increase in salt passage are observed in Figure 2a. The decrease in permeate flux and the simultaneous increases in salt passage, OUR and citrate (TOC) removal (Figure 2) indicate that biofilm formation on the membrane induces the decrease in permeate flux. Furthermore, due to biofilm growth, salt concentration is elevated in close proximity to the membrane surface consequently increasing the transmembrane osmotic pressure. In our recent study (Herzberg and Elimelech, 2007), we have shown that the simultaneous increase in transmembrane osmotic pressure and hydraulic resistance contributed by the biofouling layer decreases the permeate flux of RO membranes.

Determination of the limiting substrates for biofilm growth

Stoichiometrically, all nutrients (mainly phosphorous and nitrogen) were added in excess compared to citrate, which was supplemented as the carbon and energy source for the biofouling layer. Therefore, two substances may limit biofilm and suspended cell growth in the RO unit—oxygen and citrate. While oxygen in the feed solution is maintained at a relatively constant concentration (3.44 ± 0.02 mg l⁻¹), citrate and other nutrients are depleted due to the batch growth of the bacteria (both suspended and biofilm cells) in the RO biofouling tests. By measuring OUR by the biofouling layer together with citrate degradation rate in the feed solution (determined as TOC in Figure 2b), we can determine which of the two is limiting biofilm

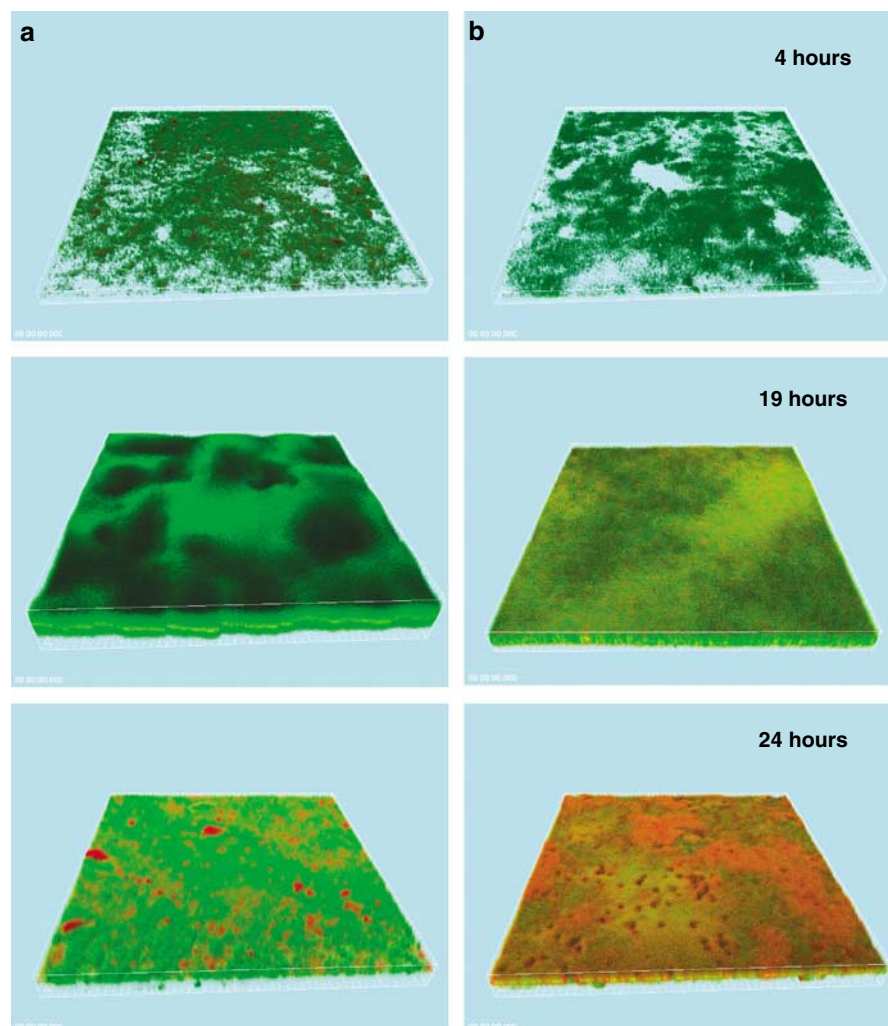


Figure 1 Three-dimensional reconstruction, using Imaris software (Bitplane, Zurich, Switzerland), of laser scanning confocal microscope (LSCM) images taken from different biofouling runs (terminated at different time points), which were supplemented with citrate as a carbon source. Planar images were acquired at depth intervals of $1\ \mu\text{m}$ (each figure is a perspective of a $750 \times 750\ \mu\text{m}$ field of view). (a, b) Biofouling layer of *P. aeruginosa* chromosomally tagged with short-life green fluorescent protein (GFP) (PAO1 AH298) and counterstained with the lectin concanavalin A conjugated to tetramethylrhodamine isothiocyanate (TRITC), and with propidium iodide (PI), respectively.

Table 1 Specific biovolume ($\mu\text{m}^3/\mu\text{m}^2$) components in *P. aeruginosa* PAO1 biofilm (obtained with COMSTAT)

Time (h)	Viable cells	Dead cells	EPS
4	3.05 ± 0.72	0.001 ± 0.00	0.35 ± 0.05
10	18.66 ± 1.51	0.31 ± 0.07	6.52 ± 1.00
19	30.85 ± 7.83	14.98 ± 4.98	4.00 ± 1.87
24	5.92 ± 2.44	15.61 ± 5.48	0.53 ± 0.22

Abbreviation: EPS, extracellular polymeric substance.

growth. After ca. 15 h of the biofouling run (or 9 h after the inoculation of bacteria), OUR by the biofilm reached its maximum value and the permeate oxygen concentration depleted to its lowest value of about $1\ \text{mg l}^{-1}$. Since citrate concentration after 15 h is still relatively high (as only about 30% of the initial TOC was degraded), it is likely that at this point oxygen is the limiting substrate for biofilm

growth. However, at this point, it is still possible that both citrate and oxygen may limit growth at some locales in the biofilm. It should be mentioned that since nitrate was not supplemented in the growth medium, *P. aeruginosa* was incapable of anoxic growth in this investigation.

Citrate seems to become a limiting substrate for growth toward the end of the fouling experiment. After 19 h of the biofouling run (Figure 2b), the TOC degradation rate was relatively low and only a minor change in TOC removal was observed during the last 5 h of the biofouling experiment. As a result of the decrease in the TOC degradation rate, the OUR by the biofilm also decreased and the permeate oxygen concentration increased. Therefore, at this point, since citrate depletion is reducing the biological oxygen demand of the media, oxygen is no longer the limiting substrate and citrate becomes the limiting substrate for biofilm growth.

Temporal response of biofilm spatial activity

By growing a biofilm-forming strain, which expresses an unstable GFP controlled by a growth-rate-dependent promoter (Werner *et al.*, 2004), we aimed at mapping the distribution of viable cells in the RO biofilm. The use of GFP to measure metabolically active zones in biofilms was reported in a variety of studies. For example, Werner *et al.*

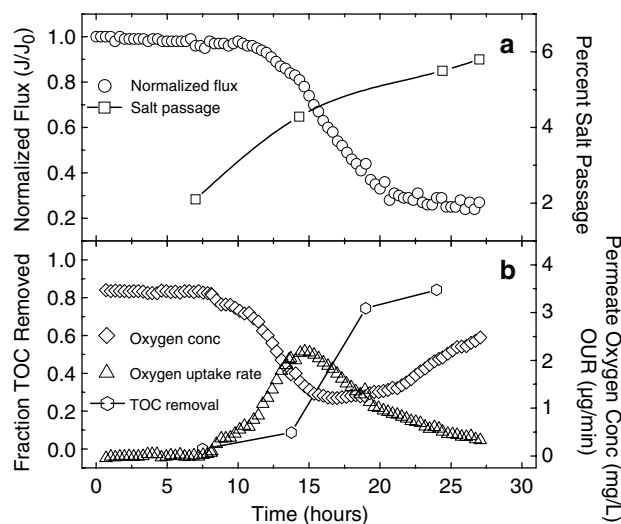


Figure 2 (a) Flux decline and increase in salt passage upon biofouling of the reverse osmosis (RO) membrane with *P. aeruginosa* PAO1. (b) Total organic carbon (TOC) removal, dissolved oxygen concentration in the permeate and oxygen uptake rate (OUR) by the biofouling layer during biofouling of the RO membrane with *P. aeruginosa* PAO1. OUR by the biofilm layer is calculated as the product of the permeate flow rate and the difference between oxygen concentration in the feed (constant value of $3.44 \pm 0.02 \text{ mg l}^{-1}$) and the permeate solution. Initial flux and TOC concentration were $1.18 \times 10^{-5} \text{ m s}^{-1}$ ($42.5 \text{ l m}^{-2} \text{ h}^{-1}$ or $25.0 \text{ gal ft}^{-2} \text{ day}^{-1}$) and $81.9 \pm 1.9 \text{ mg l}^{-1}$, respectively.

(2004) showed that partial penetration of oxygen in the biofilm results in inactive zones in *P. aeruginosa* biofilms where cells are not growing. Sternberg *et al.* (1999) observed cell growth distribution in biofilms that were grown in a flow-cell device. By using the same GFP variant, Herzberg *et al.* (2006) showed that enhanced nutrient availability in a biologically activated carbon reactor increases the viability of the attached biofilm layers. However, to date, no studies have been reported on the spatial activity of RO biofilms.

In addition to visualizing viable cells of PAO1 in the biofouling layer, dead cells were counterstained with PI. By measuring red and green pixel distribution (a percentage of the pixels in a confocal plane out of the total number of pixels in the image stack), temporal changes in the spatial GFP expression versus the location of dead bacteria were analyzed. The results are presented in Figure 3 for the various RO biofouling stages.

At 4 h after inoculating bacteria, a relatively high cell viability and a negligible amount of dead cells were observed (Figure 1b–4 h, Figure 3a and Table 1), most likely due to a high citrate concentration or low TOC removal (Figure 2). After 10 h of growth, dead cells can be distinguished (Figure 3b and Table 1) and GFP spatial distribution is located closer to the bulk liquid (Figure 3b). At this stage of the biofouling run, we presume that the high oxygen concentration ($3.44 \pm 0.02 \text{ mg l}^{-1}$) dictates higher cell viability close to the bulk liquid, since oxygen is most likely a limiting substrate for cell growth. After 19 and 24 h, GFP spatial distribution is closer to the membrane surface (Figures 3c and d). A green band in a cross section of the biofilm indicates that GFP expression is increasing close to the membrane after 19 h. Supporting these results, a higher density of

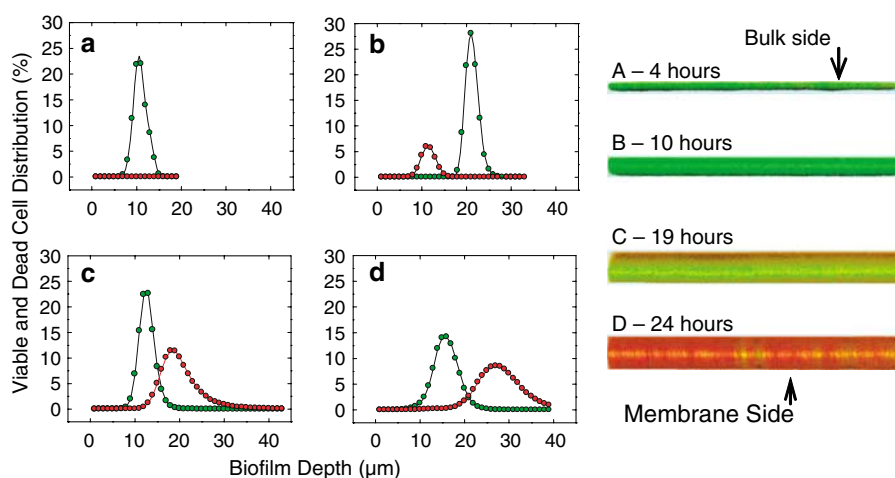


Figure 3 Distribution of red (propidium iodide (PI) as indicator for dead cells) and green (green fluorescent protein (GFP) controlled by growth-dependent promoter as indicator for viable cells) spots in the *P. aeruginosa* PAO1 biofouling layer. Cell distribution is defined as the percent of green/red pixels from the total number of pixels in all laser scanning confocal microscope (LSCM) sections of the fouling layer. The right panel describes representative cross sections of the biofouling layer at different time points. Panels a, b, c, and d correspond to the time points on the right panel. Samples were collected at the end of each experiment, which was terminated at different time points (as described in Figure 1). Analysis was obtained from COMSTAT.

PI-stained cells (dead cells) was observed close to the bulk liquid, after 19 and 24 h.

The dissolved salts, including citrate, form a polarized layer with a higher nutrient concentration within the biofilm close to the membrane surface. Since citrate is a limiting substrate for biofilm growth at this stage, more active cells are located near the membrane surface and more dead cells are found close to the bulk liquid (Figures 3c and d and corresponding cross sections). Additional evidence for the increased viability and growth rate near the membrane surface is found in the specific green fluorescence readings (excited at 488 nm) for re-suspended biofilm cells and planktonic cells taken from a 20-h-long biofouling experiment. Biofilm cells fluoresced 0.059 ± 0.013 (arbitrary intensity units) per cell, while the corresponding fluorescence for planktonic cells was 0.012 ± 0.004 .

This investigation on *P. aeruginosa* RO biofilm demonstrates a unique biofilm growth behavior compared to previous studies on the characterization of biofilm physiology. In most cases thus far, major biochemical and genetic differences in the biofilm cells are attributed to their slower growth rate compared to their associated suspended cells (Xu *et al.*, 2001; Schembri *et al.*, 2003) (in addition to the contribution of being in a sessile mode of growth). Our study shows, for the first time, that in RO biofouling, when low nutrient concentration is nearly insufficient to support extensive cell growth, the solute polarized layer near the membrane enhances cell growth to a higher degree than the suspended culture. This increased nutrient concentration near the membrane is inherent in RO membranes and is enhanced by the biofouling layer, due to 'biofilm-enhanced' concentration polarization effect (Herzberg and Elimelech, 2007).

Gene expression in P. aeruginosa biofilm grown on RO membrane

To further elucidate the physiological changes *P. aeruginosa* PAO1 cells undergo as sessile cells on the RO membrane compared to the suspended cells in the RO unit, a 20-h-long biofouling experiment using the wild-type *P. aeruginosa* PAO1 was conducted. Total RNA was extracted from both the biofilm and suspended cultures for transcriptome analysis using DNA microarray assay.

At this stage, when the transcriptome analysis was conducted, citrate was a limiting substrate for growth and a higher cell viability was observed close to the membrane surface (Figures 2 and 3). In all stages of biofilm growth described thus far in this paper, this stage is likely to be the most representative of RO unit operation under biofouling conditions. Usually, in RO units, bacteria are exposed to insufficient levels of nutrients for extensive growth. Furthermore, due to concentration polarization effects, nutrients are highly concentrated near the membrane surface. Hence, in our case, the threefold

increase in salt passage after 20 h (Figure 2) is additional proof for the substantial increase of nutrient levels in close proximity to the RO biofilm.

The *P. aeruginosa* PAO1 genome array (Affymetrix) was used to compare the transcriptomes of the biofilm and suspended cultures. In total, 278 genes were repressed in the biofilm cells more than twofold. The down-expressed genes relate to adaptation, repression of capsule synthesis, motility and attachment, chemotaxis, transport, post-translational processes, synthesis and metabolism, energy and metabolism, and genes for which a function is unknown. In total, 197 genes were induced in the RO biofilms more than twofold (see Supplementary material). The up-expressed genes relate to capsule and cell envelope, synthesis and metabolism, energy and metabolism, transport, phage, post-translational processes, and genes with an unknown function. Table 2 summarizes the genes of primary interest according to the following discussion.

Motility and attachment. Table 2 indicates that 26 genes in *P. aeruginosa* RO membrane biofilm, related to the structure and function of pili and flagella, were repressed between 2.2- and 10-fold. Such changes were already shown in the first study describing gene expression in *P. aeruginosa* biofilms by Whiteley *et al.* (2001). As in this study, by Whiteley *et al.*, our study also used a mature biofilm layer for comparison with its corresponding suspended culture. We also postulate that pili and flagella are not required for maintenance and development of a mature biofilm, as suggested by Whiteley *et al.*

Respiration. Respiratory genes PAO106, PAO105 and PAO108, which encode for cytochrome *c* oxidase subunits I, II and III, were repressed 3.2-, 2.5-, and 3.7-fold, respectively. A reduced expression of genes encoding terminal electron acceptors in the biofilm cells corresponds well with the low oxygen concentration prevailing in the biofilm (Figure 2).

Stationary phase-related genes induced in the suspended culture. Some of the differences in gene expression presented here are related to the differences in the nutritional conditions and the growth rate between the two cultures. As shown earlier in this paper, with access to a limited carbon source in the RO unit, the elevated salt (nutrient) concentration within the biofilm enhanced cell growth close to the membrane surface. The stationary-phase sigma factor RpoS is an RNA polymerase σ subunit influencing the expression of more than 700 genes in *P. aeruginosa* and has a role in cell resistance at various stress conditions (Schuster *et al.*, 2004). The transcription of *rpoS* is enhanced under stationary growth (Fujita *et al.*, 1994), and is affecting alginate biosynthesis, biofilm formation, and expression of quorum-control genes in

Table 2 Genes of interest differentially expressed in membrane-sessile cells compared to suspended cells in the RO unit

Gene	Expression ratio	Description
<i>Motility and attachment</i>		
<i>PA1077, flgB</i>	-9.8	Flagellar basal-body rod protein
<i>PA4525, pilA</i>	-9.8	Type 4 fimbrial precursor
<i>PA1080, flgE</i>	-9.2	Flagellar hook protein
<i>PA1079, flgD</i>	-8.6	Flagellar basal-body rod modification protein
<i>PA1078, flgC</i>	-7.5	Flagellar basal-body rod protein
<i>PA1082, flgG</i>	-7.5	Flagellar basal-body rod protein
<i>PA1081, flgF</i>	-7.0	Flagellar basal-body rod protein
<i>PA1086, flgK</i>	-5.7	Flagellar hook-associated protein 1
<i>PA1083, flgH</i>	-5.3	Flagellar L-ring protein precursor
<i>PA1084, flgI</i>	-4.6	Flagellar P-ring protein precursor
<i>PA1092, fliC</i>	-4.6	Flagellin type B
<i>PA1087, flgL</i>	-4.0	Flagellar hook-associated protein type 3
<i>PA1453, flhF</i>	-4.0	Flagellar biosynthesis protein
<i>PA1085, flgJ</i>	-3.7	Flagellar protein FlgJ
<i>PA1094, fliD</i>	-3.7	Flagellar capping protein
<i>PA1101, fliF</i>	-3.7	Flagellar M-ring protein
<i>PA1102, fliG</i>	-3.7	Flagellar motor switch protein
<i>PA1443, fliM</i>	-3.5	Flagellar motor switch protein
<i>PA1098, fleS</i>	-3.2	Two-component sensor
<i>PA1100, fliE</i>	-3.2	Flagellar hook-basal body complex protein
<i>PA1452, flhA</i>	-3.0	Flagellar biosynthesis protein
<i>PA1099, fleR</i>	-3.0	Two-component response regulator
<i>PA1454</i>	-3.0	Flagellar synthesis regulator, rhamnolipid related
<i>PA1444, fliN</i>	-2.3	Flagellar motor switch protein
<i>PA1445, fliO</i>	-2.5	Flagellar protein FliO
<i>PA1455, fliA</i>	-2.3	Sigma factor FliA
<i>Capsule synthesis</i>		
<i>PAO763, mucA</i>	-3.2	Anti-sigma factor MucA
<i>PAO766, mucD</i>	-3.0	Serine protease MucD precursor, secreted factors (toxins, enzymes and alginate)
<i>PA3385, amrZ</i>	-3.0	Alginate and motility regulator Z
<i>Post-translational processes</i>		
<i>PA1671, stk1</i>	3.0	Serine-threonine kinase Stk1, Stp1 is inhibited by NaF and by EDTA
<i>Synthesis and metabolism</i>		
<i>PAO740, sdsA1</i>	-14.9	Alkylsulfatase-SDS hydrolase SdsA1
<i>PA2862, lipA</i>	-5.7	Lactonizing lipase precursor, carbon compound catabolism; secreted factors (toxins,

Table 2 Continued

Gene	Expression ratio	Description
<i>PA2815</i>	-4.9	enzymes and alginate), downregulated by quorum sensing signals Probable acyl-CoA dehydrogenase
<i>PA4880</i>	-4.6	Probable bacterioferritin, iron detoxification
<i>PA5060, phaF</i>	-4.0	Polyhydroxyalkanoate synthesis protein
<i>PAO108, coIII</i>	-3.7	Cytochrome <i>c</i> oxidase, subunit III
<i>PA2550</i>	-3.7	Probable acyl-CoA dehydrogenase, fatty acid oxidation
<i>PAO106, coxA</i>	-3.2	Cytochrome <i>c</i> oxidase, subunit I, copper toxicity related
<i>PA1828</i>	-3.2	Probable short-chain dehydrogenase
<i>PA4468, sodM</i>	-3.2	Superoxide dismutase, removal of superoxide radicals
<i>PA4813, lipC</i>	-3.2	Lipase, fatty acid and phospholipid metabolism, glycerol biosynthesis
<i>PA2623, icd</i>	-3.0	Isocitrate dehydrogenase, amino-acid biosynthesis and metabolism
<i>PA2939</i>	-3.0	Probable aminopeptidase
<i>PA1199</i>	-3.0	Probable lipoprotein with prephenate L-arogenate degradation abilities
<i>PAO105, coxB</i>	-2.5	Cytochrome <i>c</i> oxidase, subunit II
<i>PA5427, adhA</i>	4.6	Alcohol dehydrogenase
<i>PA4587, ccpR</i>	3.5	Cytochrome c551 peroxidase precursor
<i>PA1279, cobU</i>	3.0	Nicotinate-nucleotide—dimethylbenzimidazole phosphoribosyltransferase (biosynthesis of cobalamin)
<i>Transcriptional regulators</i>		
<i>PA3622, rpoS</i>	-2.5	Sigma factor RpoS
<i>Adaptation</i>		
<i>PA4876, osmE</i>	-5.7	Osmotically inducible lipoprotein
<i>PA2065, pcoA</i>	-3.7	Copper resistance protein A precursor
<i>PA2064, pcoB</i>	-2.8	Copper resistance protein B precursor
<i>Cell division</i>		
<i>P00857, bolA</i>	-2.5	Morphogene protein Bola
<i>Transport</i>		
<i>PA4590, pra</i>	-4.9	Protein activator, transport of small molecules, carbon compound catabolism
<i>PA1777, oprF</i>	-3.0	Outer membrane protein precursor, transport of small molecules
<i>PA2505, opdT</i>	-3.0	Tyrosine porin
<i>PA2520, czcA</i>	-2.5	RND divalent metal cation efflux transporter CzcA
<i>PA2521, czcB</i>	-3.0	RND divalent metal cation efflux membrane fusion

Table 2 Continued

Gene	Expression ratio	Description
		protein precursor, transport of small molecules, Zinc, Cobalt, and Cadmium resistance
PA2522, <i>czcC</i>	-2.1	Outer membrane protein precursor CzcC
PA3221, <i>csaA</i>	-4.6	Protein secretion/export apparatus, molecular chaperone for exported proteins
<i>Chemotaxis</i>		
PA4309, <i>pctA</i>	-3.7	Chemotactic transducer
PA1464	-3.5	Probable purine-binding chemotaxis protein
PA4633	-3.5	Probable chemotaxis transducer
PA1423, <i>bdlA</i>	-3.2	Probable chemotaxis transducer
PA2867	-3.2	Probable chemotaxis transducer
PAO176	-2.6	Probable chemotaxis transducer
PAO177	-2	Probable purine-binding chemotaxis protein
PAO178	-2	Probable two-component sensor
PAO179	-2.1	Probable two-component response regulator
PA1456, <i>cheY</i>	-2.3	Two-component response regulator CheY
PA1457, <i>cheZ</i>	-2.3	Chemotaxis protein CheZ
PA1458	-2.8	Probable two-component sensor
PA1459	-2.6	Probable methyltransferase
PA1460	-2.1	Probable chemotaxis transmembrane proton channel
PA1561, <i>aer</i>	-2.3	Aerotaxis receptor Aer
PA1608	-2.3	Probable chemotaxis transducer
PA2652	-2.1	Probable chemotaxis transducer
PA2654	-2.3	Probable chemotaxis transducer
PA2788	-2.5	Probable chemotaxis transducer
PA3349	-2.5	Probable chemotaxis protein
PA4520	-2.3	Probable chemotaxis transducer
PA4954, <i>motA</i>	-2	Chemotaxis protein MotA

Abbreviations: RO, reverse osmosis; SDS, sodium dodecyl sulfate.

P. aeruginosa (Schuster *et al.*, 2004). The down-regulation of the *rpoS* gene in the RO biofilm (2.5-fold) is in accordance with the slower growth of the suspended cells under the nutrient-limiting conditions prevailing in the RO unit (*rpoS* is induced in the suspended cells).

In accordance with the higher citrate concentration close to the membrane surface, *icd* gene (PA2623), encoding for isocitrate dehydrogenase, was repressed threefold in the biofilm cells. This

result is consistent with those of a previous study by Chao *et al.* (1997), in which a higher growth rate of *E. coli* cells was shown to downregulate the expression of the *icd* gene.

Despite the differences in the conditions to which the suspended and biofilm cells were exposed, we did not identify changes in the expression of genes that are related to either adaptation to high osmolarity or to high hydraulic pressure (Aspedon *et al.*, 2006; Malone *et al.*, 2006). Nevertheless, *osmE*, a gene encoding for an envelope protein with an unknown function, which was reported to be induced by elevated osmolarity (Bordes *et al.*, 2000), was repressed 5.7-fold in the biofilm cells. This gene was also reported to be induced upon deceleration of growth rate and to be positively regulated by the stationary-phase sigma factor RpoS (Bordes *et al.*, 2000). The induction of *rpoS* in the suspended cells, where growth rate is decelerated, may be the reason for the induction of *osmE* in the suspended cells (repressed in the biofilm cells).

Another stationary-phase gene, *bolA*, related to cell division in *E. coli* (Lange and Hengge-Aronis, 1991), was repressed 2.5-fold in the RO biofilm (induced in the suspended cells). The induction of *bolA* is also regulated by *rpoS* (Lange and Hengge-Aronis, 1991). Overexpression of *bolA* in *E. coli* enhances biofilm formation, while deletion of *bolA* decreases biofilm formation (Vieira *et al.*, 2004). This behavior also implies that the gene expression pattern in *P. aeruginosa* biofilm grown on RO membranes follows the differences in nutritional conditions between the biofilm and the suspended cells in the unit. Also, a tyrosine porin gene, *opdT*, was repressed in the RO biofilm cells, most likely due to the higher nutrient levels within the biofilm cells. In support of this result, this specific channel for nutrient uptake, OpdT, was previously reported to be induced in *P. aeruginosa* under nutrient-limited conditions (Tamber *et al.*, 2006).

Chemotaxis. The higher availability of a carbon source to the biofilm cells in the RO unit, under the prevailing minimal citrate concentration in the bulk, exposes the suspended cells to starvation conditions in comparison to the biofilm cells. Chemotaxis proteins were induced in *P. aeruginosa* biofilm at a late maturation stage (Southey-Pillig *et al.*, 2005). Also, a chemotaxis response to starvation stimuli was reported for *Rhizobium meliloti* by Wei and Bauer (1998). In this study, since the suspended cells are exposed to a lower nutrient concentration, they are likely to induce chemotaxis genes. Thus, 22 genes related to chemotaxis were repressed 2- to 3.7-fold in the biofilm cells. It was previously reported that the expression of chemotaxis genes is positively related to *rpoS* expression, in which a set of chemotaxis genes were repressed in an *rpoS*-null mutant (Schuster *et al.*, 2004). Therefore, since *rpoS* was repressed in the biofilm cells, chemotaxis genes were also repressed. Recently, an induction of a

chemotaxis regulator, BdlA, was found to be involved in biofilm dispersion as a response to a sudden increase in nutrient concentrations (Morgan *et al.*, 2006). In our study, since nutrients are highly concentrated in the biofilm environment and since the biofilm was not yet in its detachment stage (Figure 1 and Table 1), *bdlA*, not surprisingly, was repressed 3.2-fold.

Resistance to antimicrobial agents. The low susceptibility of biofilm cells to antibiotics is generally attributed to the lower penetration rate of the antibiotics to the biofilm, and to changes in cell physiology, which are related to lower growth of the biofilm cells (Gilbert *et al.*, 1990; Stewart, 2002). These changes include stress response, higher expression of antibiotic-modifying/degrading enzymes and the presence of a sub-population of persister cells (Stewart, 2002; Shah *et al.*, 2006). For example, Whiteley *et al.* (2001) showed that a *P. aeruginosa* biofilm induces a moderate level of resistance to antimicrobial treatment through induction of *tolA* (3.9-fold) in biofilm cells. TolA is known to affect LPS structure, resulting in decreased affinity to aminoglycosides (Rivera *et al.*, 1988).

Since in this RO biofouling study biofilm cell growth is enhanced compared to the suspended cells, we were interested to examine the transcripts of genes known to affect cell resistance to antimicrobial and toxic agents. Interestingly, in our microarray data, gene clusters related to cell resistance to toxic agents were repressed in the biofilm cells. More specifically, *oprF*, which encodes for a nonspecific antibiotic resistance porin, was repressed threefold. OprF was shown to be overexpressed when the media were supplemented with kanamycin, ampicillin or tetracycline at a concentration of 10 mg l⁻¹ (Peng *et al.*, 2005). An induction of efflux pump-related genes in *P. aeruginosa* biofilms, in response to antibiotics, was recently found by others (Gillis *et al.*, 2005). However, our study is the first comparing the transcriptome of faster growing biofilm cells with their associated suspended culture. The difference in growth rate of RO biofilms may play a major role in the expression of efflux pumps in RO biofilms compared to the suspended cells in the RO unit.

The genes *czcA* and *czcB* were repressed 2.5- and 3-fold, respectively. CzcA and CzcB were reported to mediate cell resistance to cobalt, zinc and cadmium, and are probably located in the periplasm (Rensing *et al.*, 1997). The transcripts for copper resistance-mediating proteins, PcoA and PcoB, were repressed in the RO biofilm 2.8- and 3.7-fold, respectively. The copper resistance mechanism has been reported to be attributed to the sequestration of copper outside the cytoplasm (Cha and Cooksey, 1991). Also, the expression of *sodM*, which encodes for superoxide dismutase, was in contrast to its expression in recent studies of *P. aeruginosa* biofilms (Southey-Pillig

et al., 2005). *sodM* was repressed 3.2-fold in the RO membrane biofilm. Superoxide dismutase provides an antioxidant defense to the cells against the reactive oxygen intermediate, superoxide (O₂⁻) (Hassett *et al.*, 1999). Superoxide dismutase expression was induced in an early maturation stage of *P. aeruginosa* biofilm in the study by Southey-Pillig *et al.* (2005).

SDS degradation. Notably, *sdsA1*, which encodes for SDS hydrolase, an essential SDS-hydrolyzing enzyme (Hagelueken *et al.*, 2006), was repressed 15-fold in the RO biofilm. This result implies that RO biofilm cells may be more susceptible to SDS compared to cells in the suspended culture. Recently, a differentiation in susceptibility to SDS by *P. aeruginosa* biofilm cells was reported (Haagensen *et al.*, 2006). Two sub-populations in the *P. aeruginosa* biofilm were defined according to their swarming motility. It was found that the motile population, which forms the 'cap' of the biofilm colonies, was more tolerant to SDS, whereas the non-motile population, which forms the 'stalk' of the colonies, was more sensitive to SDS (Haagensen *et al.*, 2006). However, in our study, a 'flat' biofilm was formed, without any 'mushroom structures' with a 'cap-forming' sub-population. This biofilm structure may be attributed to the use of a different carbon source or to the convective permeate flow through the biofilm and the underlying RO membrane. The absence of a 'cap-forming' sub-population in the RO biofilm, together with the unique nutritional conditions prevailing in the RO biofilm, may explain the differences between our study and previous studies. In this study, biofilm cells seem to induce susceptibility to SDS, while in the study by Haagensen *et al.* (2006), 'cap-forming' biofilm populations were more resistant to SDS. Studying the effect of SDS on the physiology of *P. aeruginosa* biofilms, particularly on RO membranes, may reveal new insights into novel biofouling control strategies.

Biofilm cell motility is repressed on the RO membrane, but restored on motility plates

As expected, biofilm cells were not motile immediately after isolation from the biofouling layer and no motility halo was observed on motility plates after 6 h. In contrast, under similar conditions and cell concentration, the suspended cells were motile and the diameter of the motility halo was 26 ± 9 mm after 6 h of incubation. However, after 12 h of incubation, the biofilm cells restored their motility phenotype and the diameter of the motility halo was 28 ± 8 mm. For comparison, the suspended cells had a motility halo of 54 ± 17 mm after 12 h of incubation. These results correspond with the microarray data and confirm that *P. aeruginosa* biofilm cells indeed repress their motility genes in a sessile mode of growth on the RO membrane.

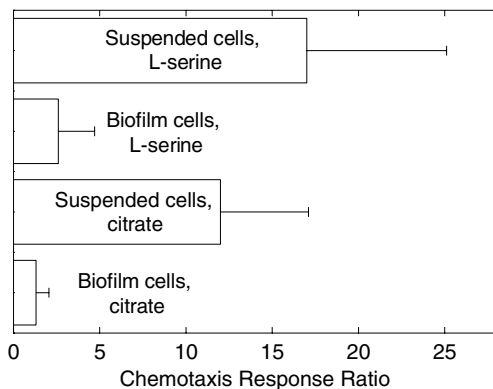


Figure 4 A 1 h chemotaxis response toward L-serine and citrate of suspended and biofilm *P. aeruginosa* cells isolated from the reverse osmosis (RO) unit. Cells were washed with secondary effluent growth media, without the carbon source. Chemotaxis response ratio was determined as the ratio of the number of the cells in the capillaries with the chemo-attractant divided by the number of cells in the absence of the chemo-attractant.

Chemotaxis response of suspended versus RO biofilm cells

Using Adler's method (Adler, 1973), chemotaxis response was higher by 12- and 17-fold in the suspended cells for L-serine and citrate, respectively (Figure 4). Interestingly, a chemotaxis-related gene cluster (PAO176, PAO177, PAO178 and PAO179) was repressed in the biofilm cells between 2- and 2.6-fold. In the study by Southey-Pillig *et al.* (2005), the gene product of PAO180, a probable chemotaxis transducer, was identified to be induced in a late matured *P. aeruginosa* biofilm. Chemotaxis genes were also induced in *P. aeruginosa* biofilms in other studies (Waite *et al.*, 2005). In this study, the increased chemotaxis response in the suspended cells corresponds to the absence of nutrients in the bulk liquid in comparison to the increased concentration of organics and electrolytes in the polarized layer near the membrane surface. Also, this phenotype supports the induction of chemotaxis genes in the suspended cells in the RO unit (Table 2). The repression of chemotaxis genes in a biofilm of *P. aeruginosa* on RO membranes is additional evidence for the unique pattern of gene expression in RO biofilms, typical of most cases in practice, when nutrients are limiting cell growth. The chemotaxis response of the suspended cells is suggested here to enhance biofouling by cells swimming toward the membrane surface in addition to cell deposition on the membrane due to permeate flux.

In conclusion, the recently proposed 'biofilm-enhanced concentration polarization' phenomenon (Herzberg and Elimelech, 2007) is shown here to affect major genetic traits in the biofouling layer of RO membranes using a model strain. Under limited access to a carbon source in the bulk liquid, faster growing cells were observed in the biofilm layer close to the membrane surface. We present the first DNA microarray data on biofilms comprising faster growing cells in comparison to the suspended

culture. Genes previously reported to be induced in laboratory *P. aeruginosa* biofilms were repressed in the RO biofilm. The repression of genes related to stress, adaptation, chemotaxis and resistance to antimicrobial agents in the RO biofilm cells raises the same question recently reported by Mikkelsen *et al.* (2007): Which physiological changes in biofilm cells relate to the aggregated mode of cell growth (or 'biofilm lifestyle'), and which are attributed to changes in environmental conditions (such as concentration polarization of nutrients adjacent to the RO membrane surface)?

Acknowledgements

Financial support for this study was provided by the WaterCAMPWS, a Science and Technology Center of Advanced Materials for the Purification of Water with Systems under the National Science Foundation agreement number CTS-0120978, and by a postdoctoral fellowship (to MH) from the United States-Israel Binational Agricultural Research and Development (BARD) fund. We are also grateful to Professor S Molin from the Technical University of Denmark for providing us with *Pseudomonas aeruginosa* PAO1 AH298.

References

- Adler J. (1973). A method for measuring chemotaxis and use of the method to determine optimum conditions for chemotaxis by *Escherichia coli*. *J Gen Microbiol* **74**: 77–91.
- Ang WS, Lee S, Elimelech M. (2006). Chemical and physical aspects of cleaning of organic-fouled reverse osmosis membranes. *J Membrane Sci* **272**: 198–210.
- Aspedon A, Palmer K, Whiteley M. (2006). Microarray analysis of the osmotic stress response in *Pseudomonas aeruginosa*. *J Bacteriol* **188**: 2721–2725.
- Boles BR, Thoendel M, Singh PK. (2005). Rhamnolipids mediate detachment of *Pseudomonas aeruginosa* from biofilms. *Mol Microbiol* **57**: 1210–1223.
- Bordes P, Repoila F, Kolb A, Gutierrez C. (2000). Involvement of differential efficiency of transcription by E σ^s and E σ^{70} RNA polymerase holoenzymes in growth phase regulation of the *Escherichia coli osmE* promoter. *Mol Microbiol* **35**: 845–853.
- Branda SS, Vik A, Friedman L, Kolter R. (2005). Biofilms: the matrix revisited. *Trends Microbiol* **13**: 20–26.
- Cha J, Cooksey D. (1991). Copper resistance in *Pseudomonas syringae* mediated by periplasmic and outer membrane proteins. *Proc Natl Acad Sci USA* **88**: 8915–8919.
- Chao G, Shen J, Tseng C, Park S, Gunsalus R. (1997). Aerobic regulation of isocitrate dehydrogenase gene (*icd*) expression in *Escherichia coli* by the *arcA* and *far* gene products. *J Bacteriol* **179**: 4299–4304.
- Costerton WJ, Lewandowski Z, Caldwell DE, Korber DR, Lappin-Scott HM. (1995). Microbial biofilms. *Annu Rev Microbiol* **49**: 711–745.
- Danese PN, Pratt LA, Dove SL, Kolter R. (2000). The outer membrane protein, Antigen 43, mediates cell-to-cell interactions within *Escherichia coli* biofilms. *Mol Microbiol* **37**: 424–432.

- Davies DG, Chakrabarty AM, Geesey GG. (1993). Exopolysaccharide production in biofilms: substratum activation of alginate gene expression by *Pseudomonas aeruginosa*. *Appl Environ Microbiol* **59**: 1181–1186.
- Davies DG, Parsek MR, Pearson JP, Iglewski BH, Costerton JW, Greenberg EP. (1998). The involvement of cell-to-cell signals in the development of a bacterial biofilm. *Science* **280**: 295–298.
- Donlan RM. (2002). Biofilms: microbial life on surfaces. *Emerging Infect Dis* **8**: 881–890.
- Drenkard E. (2003). Antimicrobial resistance of *Pseudomonas aeruginosa* biofilms. *Microbes Infect* **5**: 1213–1219.
- Friedman L, Kolter R. (2004). Two genetic loci produce distinct carbohydrate-rich structural components of the *Pseudomonas aeruginosa* biofilm matrix. *J Bacteriol* **186**: 4457–4465.
- Fujita M, Tanaka K, Takahashi H, Amemura A. (1994). Transcription of the principal sigma-factor genes, *rpoD* and *rpoS*, in *Pseudomonas aeruginosa* is controlled according to the growth phase. *Mol Microbiol* **13**: 1071–1077.
- Gilbert P, Collier PJ, Brown MR. (1990). Influence of growth rate on susceptibility to antimicrobial agents: biofilms, cell cycle, dormancy, and stringent response. *Antimicrob Agents Chemother* **34**: 1865–1868.
- Gillis RJ, White KG, Choi K-H, Wagner VE, Schweizer HP, Iglewski BH. (2005). Molecular basis of azithromycin-resistant *Pseudomonas aeruginosa* biofilms. *Antimicrob Agents Chemother* **49**: 3858–3867.
- Haagensen JAJ, Klausen M, Ernst RK, Miller SI, Folkesson A, Tolker-Nielsen T *et al.* (2006). Differentiation and distribution of colistin/SDS tolerant cells in *Pseudomonas aeruginosa* biofilms. *J Bacteriol* **189**: 28–37.
- Hagelueken G, Adams TM, Wiehlmann L, Widow U, Kolmar H, Tummeler B *et al.* (2006). The crystal structure of SdsA1, an alkylsulfatase from *Pseudomonas aeruginosa*, defines a third class of sulfatases. *Proc Natl Acad Sci USA* **103**: 7631–7636.
- Hammer BK, Bassler BL. (2003). Quorum sensing controls biofilm formation in *Vibrio cholerae*. *Mol Microbiol* **50**: 101–104.
- Hassett DJ, Elkins JG, Ma J-F, McDermott TR. (1999). *Pseudomonas aeruginosa* biofilm sensitivity to biocides: use of hydrogen peroxide as model antimicrobial agent for examining resistance mechanisms. *Methods Enzymol* **310**: 599–608.
- Herzberg M, Dosoretz CG, Kuhn J, Klein S, Green M. (2006). Visualization of active biomass distribution in a BGAC fluidized bed reactor using GFP tagged *Pseudomonas putida* F1. *Water Res* **40**: 2704–2712.
- Herzberg M, Elimelech M. (2007). Biofouling of reverse osmosis membranes: role of biofilm-enhanced osmotic pressure. *J Membrane Sci* **295**: 11–20.
- Heydorn A, Nielsen AT, Hentzer M, Sternberg C, Givskov M, Ersboll BK *et al.* (2000). Quantification of biofilm structures by the novel computer program COMSTAT. *Microbiology* **146**: 2395–2407.
- Jackson KD, Starkey M, Kremer S, Parsek MR, Wozniak DJ. (2004). Identification of *psl*, a locus encoding a potential exopolysaccharide that is essential for *Pseudomonas aeruginosa* PAO1 biofilm formation. *J Bacteriol* **186**: 4466–4475.
- Kirisits MJ, Parsek MR. (2007). Does *Pseudomonas aeruginosa* use intercellular signalling to build biofilm communities? *Cell Microbiol* **8**: 1841–1849.
- Lange R, Hengge-Aronis R. (1991). Growth phase-regulated expression of *bolA* and morphology of stationary-phase *Escherichia coli* cells are controlled by the novel sigma factor sigma S. *J Bacteriol* **173**: 4474–4481.
- Liu Z, Stirling FR, Zhu J. (2007). Temporal quorum-sensing induction regulates *Vibrio cholerae* biofilm architecture. *Infect Immun* **75**: 122–126.
- Malone AS, Chung Y-K, Yousef AE. (2006). Genes of *Escherichia coli* O157:H7 that are involved in high-pressure resistance. *Appl Environ Microbiol* **72**: 2661–2671.
- Mikkelsen H, Duck Z, Lilley KS, Welch M. (2007). Interrelationships between colonies, biofilms, and planktonic cells of *Pseudomonas aeruginosa*. *J Bacteriol* **189**: 2411–2416.
- Morgan R, Kohn S, Hwang S-H, Hassett DJ, Sauer K. (2006). BdlA, a chemotaxis regulator essential for biofilm dispersion in *Pseudomonas aeruginosa*. *J Bacteriol* **188**: 7335–7343.
- O'Toole GA, Kaplan HB, Kolter R. (2000). Biofilm formation as microbial development. *Annu Rev Microbiol* **54**: 49–79.
- O'Toole GA, Kolter R. (1998). Flagellar and twitching motility are necessary for *Pseudomonas aeruginosa* biofilm development. *Mol Microbiol* **30**: 295–304.
- Parsek MR, Greenberg EP. (2005). Sociomicrobiology: the connections between quorum sensing and biofilms. *Trends Microbiol* **13**: 27–33.
- Peng X, Xu C, Ren H, Lin X, Wu L, Wang S. (2005). Proteomic analysis of the sarcosine-insoluble outer membrane fraction of *Pseudomonas aeruginosa* responding to ampicillin, kanamycin, and tetracycline resistance. *J Proteome Res* **4**: 2257–2265.
- Pettygrove GS, Asano T. (1984). *Irrigation with reclaimed municipal wastewater: a guidance manual*. California State Water Resources Control Board: Sacramento, CA (<http://cee.engr.ucdavis.edu/Faculty/asano/IrrigationReuse1.pdf>).
- Ramsey MM, Whiteley M. (2004). *Pseudomonas aeruginosa* attachment and biofilm development in dynamic environments. *Mol Microbiol* **53**: 1075–1087.
- Rensing C, Pribyl T, Nies D. (1997). New functions for the three subunits of the CzcCBA cation-proton antiporter. *J Bacteriol* **179**: 6871–6879.
- Ridgway HF, Flemming H-C. (1996). *Membrane Biofouling in Water Treatment Membrane Processes*. In: *Water Treatment Membrane Processes*. McGraw-Hill, New York.
- Rivera M, Hancock RE, Sawyer JG, Haug A, McGroarty EJ. (1988). Enhanced binding of polycationic antibiotics to lipopolysaccharide from an aminoglycoside-supersusceptible, *tolA* mutant strain of *Pseudomonas aeruginosa*. *Antimicrob Agents Chemother* **32**: 649–655.
- Romeo T. (2006). When the party is over: a signal for dispersal of *Pseudomonas aeruginosa* biofilms. *J Bacteriol* **188**: 7325–7327.
- Sauer K, Camper AK. (2001). Characterization of phenotypic changes in *Pseudomonas putida* in response to surface-associated growth. *J Bacteriol* **183**: 6579–6589.
- Sauer K, Camper AK, Ehrlich GD, Costerton JW, Davies DG. (2002). *Pseudomonas aeruginosa* displays multiple phenotypes during development as a biofilm. *J Bacteriol* **184**: 1140–1154.
- Sauer K, Cullen MC, Rickard AH, Zeef LAH, Davies DG, Gilbert P. (2004). Characterization of nutrient-induced dispersion in *Pseudomonas aeruginosa* PAO1 biofilm. *J Bacteriol* **186**: 7312–7326.

- Schembri MA, Christiansen G, Klemm P. (2001). FimH-mediated autoaggregation of *Escherichia coli*. *Mol Microbiol* **41**: 1419–1430.
- Schembri MA, Kjærgaard K, Klemm P. (2003). Global gene expression in *Escherichia coli* biofilms. *Mol Microbiol* **48**: 253–267.
- Schuster M, Hawkins AC, Harwood CS, Greenberg EP. (2004). The *Pseudomonas aeruginosa* RpoS regulon and its relationship to quorum sensing. *Mol Microbiol* **51**: 973–985.
- Shah D, Zhang Z, Khodursky A, Kaldalu N, Kurg K, Lewis K. (2006). Persisters: a distinct physiological state of *E. coli*. *BMC Microbiol* **6**: 53.
- Southey-Pillig CJ, Davies DG, Sauer K. (2005). Characterization of temporal protein production in *Pseudomonas aeruginosa* biofilms. *J Bacteriol* **187**: 8114–8126.
- Sperandio V, Torres AG, Kaper JB. (2002). Quorum sensing *Escherichia coli* regulators B and C (QseBC): a novel two-component regulatory system involved in the regulation of flagella and motility by quorum sensing in *Escherichia coli*. *Mol Microbiol* **43**: 809–821.
- Sternberg C, Christensen BB, Johansen T, Toftgaard Nielsen A, Andersen JB, Givskov M *et al.* (1999). Distribution of bacterial growth activity in flow-chamber biofilms. *Appl Environ Microbiol* **65**: 4108–4117.
- Stewart PS. (2002). Mechanisms of antibiotic resistance in bacterial biofilms. *Int J Med Microbiol* **292**: 107–113.
- Strathmann M, Wingender J, Flemming H-C. (2002). Application of fluorescently labelled lectins for the visualization and biochemical characterization of polysaccharides in biofilms of *Pseudomonas aeruginosa*. *J Microbiol Methods* **50**: 237–248.
- Tamber S, Ochs MM, Hancock REW. (2006). Role of the novel OprD family of porins in nutrient uptake in *Pseudomonas aeruginosa*. *J Bacteriol* **188**: 45–54.
- Vieira HLA, Freire P, Arraiano CM. (2004). Effect of *Escherichia coli* morphogene *bolA* on biofilms. *Appl Environ Microbiol* **70**: 5682–5684.
- Vrijenhoek EM, Hong S, Elimelech M. (2001). Influence of membrane surface properties on initial rate of colloidal fouling of reverse osmosis and nanofiltration membranes. *J Membrane Sci* **188**: 115–128.
- Waite R, Paccanaro A, Papakonstantinou A, Hurst J, Saqi M, Littler E *et al.* (2006). Clustering of *Pseudomonas aeruginosa* transcriptomes from planktonic cultures, developing and mature biofilms reveals distinct expression profiles. *BMC Genomics* **7**: 162.
- Waite RD, Papakonstantinou A, Littler E, Curtis MA. (2005). Transcriptome analysis of *Pseudomonas aeruginosa* growth: comparison of gene expression in planktonic cultures and developing and mature biofilms. *J Bacteriol* **187**: 6571–6576.
- Wang X, Preston III JF, Romeo T. (2004). The *pgaABCD* locus of *Escherichia coli* promotes the synthesis of a polysaccharide adhesin required for biofilm formation. *J Bacteriol* **186**: 2724–2734.
- Wei X, Bauer WD. (1998). Starvation-induced changes in motility, chemotaxis, and flagellation of *Rhizobium meliloti*. *Appl Environ Microbiol* **64**: 1708–1714.
- Werner E, Roe F, Bugnicourt A, Franklin MJ, Heydorn A, Molin S *et al.* (2004). Stratified growth in *Pseudomonas aeruginosa* biofilms. *Appl Environ Microbiol* **70**: 6188–6196.
- Whiteley M, Bangera MG, Bumgarner RE, Parsek MR, Teitzel GM, Lory S *et al.* (2001). Gene expression in *Pseudomonas aeruginosa* biofilms. *Nature* **413**: 860–864.
- Winsor GL, Lo R, Sui SJH, Ung KSE, Huang S, Cheng D *et al.* (2005). *Pseudomonas aeruginosa* Genome Database and PseudoCAP: facilitating community-based, continually updated, genome annotation. *Nucleic Acids Res* **33**: D338–D343.
- Xu KD, Franklin MJ, Park C-H, McFeters GA, Stewart PS. (2001). Gene expression and protein levels of the stationary phase sigma factor, RpoS, in continuously-fed *Pseudomonas aeruginosa* biofilms. *FEMS Microbiol Lett* **199**: 67–71.

Supplementary Information accompanies the paper on The ISME Journal website (<http://www.nature.com/ismej>)